

**FUNCTIONALIZED MULTI-WALLED CARBON
NANOTUBE/CELLULOSE ACETATE MIXED MATRIX
MEMBRANE FOR CO₂/N₂ SEPARATION**

ZEINAB ABBAS JAWAD

UNIVERSITI SAINS MALAYSIA

2014

**FUNCTIONALIZED MULTI-WALLED CARBON
NANOTUBE/CELLULOSE ACETATE MIXED MATRIX
MEMBRANE FOR CO₂/N₂ SEPARATION**

by

ZEINAB ABBAS JAWAD

**Thesis submitted in fulfillment of the
requirements for the degree of
Doctor of Philosophy**

August 2014

ACKNOWLEDGEMENT

First of all, my profound gratitude goes to the Almighty God for His divine purpose. He helped to not only quicken, sustain, and strengthen me but also kept me stable throughout all the difficult situations during the period of my PhD study.

It is my great pleasure to express my deepest appreciation and gratitude to Prof. Abdul Latif Ahamd for his advice, guidance and financial support towards this research. I would also like to extend my heartfelt gratitude to Dr. Low Siew Chun for sharing her excellent scientific knowledge, valuable suggestions, moral support, and encouragement throughout this research. I thank her for treating me as one of her own students, and to her honest soul as a great scientist. She had overcome everything even though I am from a different country, religion, and culture. Also, special thanks to Asst. Prof. Sharif Hussein Sharif Zein for sharing his great experience in the field of nanotechnology and carbon nanotubes. His advices have corrected the project steps successfully.

My sincere thanks to my group of colleagues whom I consider as my second family since I was far away from my family and friends. My deepest gratitude to them for accepting me as one of them, and supporting me during the good and bad times. I would also like to thank them for reducing my stress, whilst giving them crazy times, and sharing their knowledge. My tears drop whenever I remember them. They are Huey Ping, Swee Pin, Li Peng, Qi Hwa, Jing Yao, Bee Wah, Pey Yi, Siti Salwa, and Dr. Chew. In addition, I wish to express my appreciation to my Iraqi community who supported me at all times and provided their guidance in Malaysia especially, my cousin Mohammed Kassim and my friends Dr. Ekhlis Kadhium, Dr. Menal Hamdi, Mr. Harith, and Mr. Abdullah.

My thanks to all the technicians and staff of the School of Chemical Engineering for their cooperation especially, Encik Shamsul and his brother Encik Abda who helped me in the fabrication of the experimental rig used in this project. I would also like to acknowledge the staff from the Nanotechnology and Advance Materials Research Center/ University of Technology especially, Prof. Adwayia Haider, Ms. Zainab Naser and Mss. Allaa Abdul Jabbar.

My special thanks to the University of Technology-Iraq for the financial support awarded, to pursue my studies. In addition, I wish to acknowledge the financial support granted by the MOSTI Science Fund (Grant no: 305/PJKIMIA/6013386), FRGS (Grant no: 203/PJKIMIA/6071234), RU-PRGS (Grant no: 1001/PJKIMIA/8045029), and Universiti Sains Malaysia RU Membrane Science and Technology Cluster.

Last but not least, I would like to express my heartfelt appreciation and love to my wonderful aunts, uncles, and cousins for their immense sacrifices and support throughout my life. Without their prayers, encouragement, and advice, it would have been a difficult task to achieve my dreams. To the souls of my lovely parents, I hope you would have been proud of me if you were still amongst us today. Finally, I would like to take this opportunity to say although I may not be the best in this field, I have certainly given my best towards this research. Further, from the bottom of my heart, I hope someday we will synthesize a membrane, which can separate our happiness from our sadness.

Zeinab Abbas Jawad

August 2014

TABLE OF CONTENTS

	Page
ACKNOWLEDGEMENT	ii
TABLE OF CONTENTS	iv
LIST OF TABLES	x
LIST OF FIGURES	xiii
LIST OF PLATES	xviii
LIST OF ABBREVIATIONS	xx
LIST OF SYMBOLS	xxiii
ABSTRAK	xxv
ABSTRACT	xxvii
CHAPTER ONE– INTRODUCTION	
1.1 Global Issues of Carbon Dioxide as a Greenhouse Gas	1
1.2 Membrane Gas Separation	2
1.3 Mixed Matrix Membrane (MMM)	3
1.4 Importance of MMM	4
1.5 Problem Statement	6
1.6 Research Objectives	8
1.7 Research Scope	9
1.8 Organization of Thesis	11

CHAPTER TWO – LITERATURE REVIEW

2.1	The Global Issues of Greenhouse Gas	14
2.1.1	The Effects of Greenhouse Gas	14
2.1.2	The Removal of CO ₂	16
2.1.2 (a)	Chemical Absorption Method	18
2.1.2 (b)	Membrane Gas Separation	20
2.2	MMM-CNTs for Gas Separation	22
2.2.1	Physical and Chemical Properties of MMM	24
2.2.2	Synthesize of MMM	26
2.2.3	Challenges in MMM Synthesis	28
2.3	Asymmetric Polymeric Membrane in Synthesize MMM	29
2.3.1	Chemical and Physical Properties of Polymer Matrix	30
2.3.2	Effect of Membrane Composition	32
2.3.2 (a)	Polymer Concentration	32
2.3.2 (b)	Solvent	33
2.3.3	Casting Condition	34
2.3.4	Drying Method of CA Membrane	34
2.3.4 (a)	Vacuum Drying Method	35
2.3.4 (b)	Solvent-Exchange Drying Method	35
2.4	Inorganic Fillers	36
2.4.1	Properties of CNTs	39
2.4.2	Advantages and Disadvantages of CNTs	41
2.4.3	Functionalization of CNTs	42
2.4.3 (a)	Covalent Functionalization of CNTs	42
2.4.3 (b)	Non-Covalent Functionalization of CNTs	43

2.5	Future Direction	47
-----	------------------	----

CHAPTER THREE – KINETIC SORPTION MODEL

3.1	Model Assumption	48
3.2	Model Development	49
3.3	Model in Explaining Gas Permeation	57
3.4	Transport Mechanism in Gas Separation Membrane	59
3.4.1	Knudsen Diffusion	60
3.4.2	Molecular Sieving	61
3.4.3	Solution-Diffusion Mechanism	63

CHAPTER FOUR – MATERIALS AND METHODS

4.1	Overall Experimental Flow Chart	65
4.2	Materials and Chemicals	67
4.3	Functionalization of MWCNTs	68
4.3.1	Wrapping of β -CD around MWCNTs	68
4.3.2	The Improvement Dispersion of β -CD by Different Non-Aqueous Media Dispersing	69
4.3.3	Stability of the Functionalized MWCNTs	69
4.4	Synthesis Cellulose Acetate Membrane (CA-M)	70
4.4.1	Effect of Casting Thickness	72
4.4.2	Effect of Polymer Concentration	73
4.4.3	Effect of Drying Method	74

4.5	Development of Mixed Matrix Membrane (MMM)	74
4.5.1	Integration of MWCNTs into CA Polymer	74
4.5.2	Effect of Concentration Loadings of MWCNTs-F into the CA Polymer	76
4.5.3	Solvent Exchange Drying Method in Changing Membrane Morphologies	77
	4.5.3 (a) Effect of Exchange Time of Hexane	77
	4.5.3 (b) Effect of Exchange Time of Ethanol	77
4.6	Characterization Studies	79
4.6.1	Fourier Transform Infrared Spectroscopy (FTIR)	79
4.6.2	Raman Spectroscopy	80
4.6.3	Transmission Electron Microscopy (TEM)	80
4.6.4	Dynamic Light Scattering (DLS)	81
4.6.5	Thermogravimetric Analysis (TGA)	82
4.6.6	X-Ray Diffraction (XRD)	82
4.6.7	Nitrogen Adsorption-Desorption Measurement	83
4.6.8	Field Emission Scanning Electron Microscopy (FESEM)	83
4.6.9	Atomic Force Microscope (AFM)	83
4.6.10	Rheological Property of Membrane Doping Solution	84
4.6.11	Mechanical Properties	84
4.6.12	Bounded Water Content (BWC)	85
4.6.13	Sorption Study	85
4.7	Gas Permeation and Separation Studies	86
4.7.1	Gas Permeation and Separation Test Rig Set Up	86
4.7.2	Gas Permeation Cell	89

4.7.3	Operation of Gas Permeation and Separation Test Rig Set Up	91
	4.7.3 (a) Single Gas Permeation	91
	4.7.3 (b) Binary Gas Permeation	92
4.8	Gas Permeation and Separation Performance Studies	92
4.9	Gas Samples Analysis	93
CHAPTER FIVE – RESULTS AND DISCUSSION		
5.1	Functionalization of MWCNTs	96
	5.1.1 Properties of MWCNTs-P	96
	5.1.2 Wrapping of β -CD around MWCNTs	99
	5.1.3 The Improvement Dispersion of β -CD by Different non-aqueous Media Dispersing	109
	5.1.4 Stability of the Functionalized MWCNTs	116
5.2	Synthesis Cellulose Acetate Membrane (CA-M)	119
	5.2.1 Effect of Membrane Casting Thickness	119
	5.2.2 Effect of Polymer Concentration	124
	5.2.3 Effect of Drying Methods	128
5.3	Development of Mixed Matrix Membrane (MMM)	135
	5.3.1 Integration of MWCNTs into CA Polymer	135
	5.3.2 Effect of MWCNTs-F1 Loading Concentration	144
	5.3.3 Solvent Exchange Drying Method in Changing Membrane Morphologies	157
	5.3.3 (a) Effect of Exchange Time of Hexane	157
	5.3.3 (b) Effect Of Exchange Time of Ethanol	163

5.4	Kinetic Sorption Study	168
5.4.1	Effect of Exchange Time of Hexane	168
5.4.2	Effect of Exchange Time of Ethanol	173
5.5	Permeation and Separation Performance of CO ₂ /N ₂ Binary Gas Mixture	177
CHAPTER SIX – CONCLUSIONS AND RECOMMENDATIONS		
6.1	Conclusions	183
6.2	Recommendations	186
REFERENCES		188
APPENDICES		
Appendix A	Sample of Calculation for the Kinetic Sorption Study for the MMM Dried with 4 hrs Ethanol then 1 hr n-Hexane	208
Appendix B	Sample of Calculation of the Single Gas Permeation and Separation Performance of the MMM	210
Appendix C	GC Calibration Curve for CO ₂ and N ₂ Gases	212
Appendix D	Sample of Calculation of the Binary Gas Permeation and Separation Performance of the MMM	213
LIST OF PUBLICATIONS		217

LIST OF TABLES

		Page
Table 1.1	Comparison of the properties for polymeric, inorganic and MMM (Ismail <i>et al.</i> , 2009)	5
Table 2.1	Summary of MMMs developed using different fillers	24
Table 2.2	Physical properties of SWCNTs and MWCNTs (Ma <i>et al.</i> , 2010)	41
Table 3.1	Molecular weight and kinetic diameter of gases (Scholes <i>et al.</i> , 2008)	60
Table 4.1	List of materials and chemicals used	67
Table 4.2	The composition of membrane prepared at different casting thickness	72
Table 4.3	The composition of membrane prepared at different polymer concentration	73
Table 4.4	The composition of membrane fabrication	75
Table 4.5	The composition of membrane fabricated at different concentration loadings of MWCNTs-F1	76
Table 4.6	List of synthesized membranes in this study	78
Table 4.7	List of components of experimental rig set-up	87
Table 5.1	I_D/I_G values of MWCNTs-P, MWCNTs-F1, MWCNTs-F2, and MWCNTs-F3	102
Table 5.2	U_E values of MWCNTs-P, MWCNTs-F1, MWCNTs-F2, and MWCNTs-F3	106
Table 5.3	I_D/I_G values of MWCNTs-P, MWCNTs-F1, MWCNTs-F4, and MWCNTs-F5	110
Table 5.4	U_E values of MWCNTs-P, MWCNTs-F1, MWCNTs-F4, and MWCNTs-F5	115
Table 5.5	CO ₂ /N ₂ permeation rate and selectivity of membrane with casting thickness of 300 μ m (M2), 250 μ m (M3), and 150 μ m (M4)	121

Table 5.6	CO ₂ /N ₂ permeation rate and selectivity of membrane prepared at polymer concentration of 10 wt% (M3) and 15 wt% (M5) with casting thickness of 250 μm	126
Table 5.7	Summary of CO ₂ /N ₂ permeation properties achieved by the present work compared to other research works	135
Table 5.8	CO ₂ /N ₂ permeance rate and selectivity of as spun CA membrane (M7), mixed matrix membrane with MWCNTs-P (MMM-0.1P), and mixed matrix membrane with MWCNTs-F1 (MMM-0.1F)	142
Table 5.9	Summary of BET results	143
Table 5.10	Effect of MWCNTs-F1 loading on membrane dopes viscosity	148
Table 5.11	The mechanical properties of the membranes	154
Table 5.12	Summary of CO ₂ /N ₂ permeation properties achieved from the present work compared to previous study	156
Table 5.13	Physical properties of water, acetic acid, ethanol, and hexane (Snyder, 1974; Wohlfarth, 1997; Cheremisinoff, 2003)	158
Table 5.14	Bonded water content of MMM at vacuum drying and solvent-exchange with different exchange times of hexane	160
Table 5.15	Bonded water content of MMM at vacuum drying and solvent-exchange with different exchange times of ethanol	164
Table 5.16	CO ₂ diffusion coefficient of MMMs dried using conventional vacuum drying method and solvent-exchange approaches at different exchange times of hexane	170
Table 5.17	Hansen solubility parameters (Hansen, 1999; Romero <i>et al.</i> , 2009)	172
Table 5.18	CO ₂ diffusion coefficient of MMMs dried using conventional vacuum drying method and solvent-exchange approaches at different exchange times of ethanol	175
Table 5.19	Hansen solubility parameters (Hansen, 1999; Romero <i>et al.</i> , 2009)	176
Table 5.20	Comparison of pure and mixed gas experiments for MMM of 0.1 wt% of MWCNTs-F1 and 4 hrs ethanol followed by 1 hr n-hexane exchange drying	182

Table A.1	Measurement of the amount of CO ₂ record by TGA	208
Table A.2	Measurement of time and M_t/M_∞	208
Table B.1	Measurement of permeate stream flow using bubble flow meter	210
Table B.2	Calculated single gas fluxes and permeances	211
Table D.1	Flow and Composition of different streams in the CO ₂ /N ₂ binary gas mixture system	213

LIST OF FIGURES

		Page
Figure 1.1	MMMs in configuration: (a) symmetric flat dense, and (b) Asymmetric hollow fiber (Goh <i>et al.</i> , 2011)	4
Figure 2.1	Process flow diagram of amine separation process (Force, 2009)	19
Figure 2.2	The basic concept of membrane gas separation (Ismail <i>et al.</i> , 2009)	21
Figure 2.3	Robeson plot, trade-off curves for glassy (dotted line) and rubbery (bold dotted line) polymers are taken as the upper bound for polymer membrane separation ability; points represent a collection of experimental selectivity/permeability data for CO ₂ /N ₂ mixtures (Favre, 2007)	25
Figure 2.4	The methods to synthesize the MMM (Aroon <i>et al.</i> , 2010)	27
Figure 2.5	Schematic diagram of an ideal MMM (Aroon <i>et al.</i> , 2010)	28
Figure 2.6	Schematic diagram of an interface void in the polymer-particle interface (Aroon <i>et al.</i> , 2010)	30
Figure 2.7	The chemical structure of CA (Jie <i>et al.</i> , 2004)	31
Figure 2.8	Schematic diagram of a rigidified polymer layer in the polymer-particle interface (Aroon <i>et al.</i> , 2010)	38
Figure 2.9	TEM images of different CNTs: (a) SWCNTs and (b) MWCNTs (Lijima, 1991; Bethune <i>et al.</i> , 1993)	40
Figure 2.10	Schematic diagram illustrating the surfactant adsorption of non-covalent functionalization of CNTs (Kim, 2011)	43
Figure 2.11	Schematic diagram illustrating the endohedral method of non-covalent functionalization of CNTs (Kim, 2011)	44
Figure 2.12	Schematic diagram illustrating the polymer wrapping of non-covalent functionalization of CNTs (Kim, 2011)	45
Figure 2.13	The chemical structure of β -CD (Del Valle, 2004)	46
Figure 3.1	Schematic diagram of the gas permeation through the MMM	48

Figure 3.2	Schematic diagram represented the original concentration profile as sum of sine terms (Jackson, 2006)	52
Figure 3.3	Schematic diagram representing Knudson diffusion (Scholes <i>et al.</i> , 2008)	60
Figure 3.4	Schematic diagram representing the molecular sieving mechanism (Scholes <i>et al.</i> , 2008)	62
Figure 3.5	Schematic diagram representing the solution-diffusion mechanism (Scholes <i>et al.</i> , 2008)	64
Figure 4.1	Flowchart of overall experimental works	66
Figure 4.2	Sorption study profiles	86
Figure 4.3	Schematic diagram of the experimental rig set-up	88
Figure 4.4	Schematic diagram of the gas permeation cell	91
Figure 5.1	FTIR spectra of MWCNTs-P	96
Figure 5.2	Raman spectra of MWCNTs-P	98
Figure 5.3	FTIR spectra of MWCNTs at different β -CD concentration of (a) 0 wt% (MWCNTs-P), (b) 30 wt% (MWCNTs-F1), (c) 20 wt% (MWCNTs-F2), and (d) 10 wt% (MWCNTs-F3)	100
Figure 5.4	Raman spectra of MWCNTs at different β -CD concentration of (a) 0 wt% (MWCNTs-P), (b) 30 wt% (MWCNTs-F1), (c) 20 wt% (MWCNTs-F2), and (d) 10 wt% (MWCNTs-F3)	103
Figure 5.5	Diameter distribution for MWCNTs at different β -CD concentration of (a) 0 wt% (MWCNTs-P), (b) 30 wt% (MWCNTs-F1), (c) 20 wt% (MWCNTs-F2), and (d) 10 wt% (MWCNTs-F3)	105
Figure 5.6	TGA curves of MWCNTs at different β -CD concentration of (a) 0 wt% (MWCNTs-P), (b) - (β -CD), (c) 30 wt% (MWCNTs-F1), (d) 20 wt% (MWCNTs-F2), and (e) 10 wt% (MWCNTs-F3)	107
Figure 5.7	XRD patterns of MWCNTs at different β -CD concentration of (a) 0 wt % (MWCNTs-P), (b) - (β -CD), (c) 30 wt % (MWCNTs-F1), (d) 20 wt% (MWCNTs-F2), and (e) 10 wt% (MWCNTs-F3). Symbols: * Cage-type	108

Figure 5.8	Raman spectra of MWCNTs at different non-aqueous media of (a) - (MWCNTs-P), (b) ethanol (MWCNTs-F1), (c) acetic acid (MWCNTs-F4), and (d) water (MWCNTs-F5)	110
Figure 5.9	Schematic representation of the MWCNTs-F with β -CD and MWCNTs in solvents of different polarity	111
Figure 5.10	Diameter distribution for MWCNTs at different non-aqueous media of (a) ethanol (MWCNTs-F1), (b) acetic acid (MWCNTs-F4), and (c) water (MWCNTs-F5)	114
Figure 5.11	XRD patterns of MWCNTs at different non-aqueous media of (a) ethanol (MWCNTs-F1), (b) acetic acid (MWCNTs-F4), and (c) water (MWCNTs-F5). Symbols: * Cage-type	116
Figure 5.12	Diameter distribution for MWCNTs-F1 (a,b) without washing, and (c,d) with three repeated washing steps	118
Figure 5.13	AFM morphologies of the membrane surface with casting thickness of (a) 300 μm (M2), (b) 250 μm (M3), and (c) 150 μm (M4)	123
Figure 5.14	AFM morphologies of membrane surface fabricated at polymer concentration of (a) 7 wt% (M1), (b) 10 wt% (M3), and (c) 15 wt% (M5) with casting thickness of 250 μm	128
Figure 5.15	Schematic representing the effects of (a) conventional vacuum drying method and (b) solvent-exchange drying method ((c) immersed the membrane in non-solvent (ethanol), (d) the immersion in the second volatile solvent (hexane), and (e) the evaporation of hexane	131
Figure 5.16	AFM roughness measurement for membranes dried with (a) conventional vacuum drying method (M3) and (b) solvent-exchange drying method (M7)	132
Figure 5.17	Single gas permeances of (a) CO_2 and (b) N_2 through membranes with conventional vacuum drying (M3) and solvent-exchange drying (M7) as a function of pressure difference	133
Figure 5.18	Ideal selectivity of CO_2/N_2 through membranes with conventional vacuum drying (M3) and solvent-exchange drying (M7) as a function of pressure difference	134
Figure 5.19	Schematic representing effects of integrating MWCNTs-P into the polymer matrix	136

Figure 5.20	XRD patterns of (a) as-spun CA membrane (M7), (b) mixed matrix membrane with MWCNTs-P (MMM-0.1P), and (c) mixed matrix membrane with MWCNTs-F1 (MMM-0.1F)	140
Figure 5.21	Schematic representing effects of (a) functionalization on the MWCNTs-P structure, (b) integrating moderate amount of MWCNTs-F1 within the polymer matrix, and (c) integrating high amounts of MWCNTs-F1 among the polymer matrix	147
Figure 5.22	Single gas permeances of (a) CO ₂ and (b) N ₂ through mixed matrix membrane at different MWCNTs-F1 loadings of 0.05 wt%, 0.1 wt%, and 0.2 wt%	150
Figure 5.23	Ideal selectivity of CO ₂ /N ₂ through mixed matrix membrane at different MWCNTs-F1 loadings of 0.0 wt%, 0.05 wt%, 0.1 wt%, and 0.2 wt%	151
Figure 5.24	XRD patterns of mixed matrix membrane at different MWCNTs-F1 loading of (a) 0.05 wt%, (b) 0.1 wt%, and (c) 0.2 wt%	153
Figure 5.25	Single gas permeances (GPU) of (a) CO ₂ , (b) N ₂ gas for membranes dried using vacuum drying (M8) and solvent-exchange approaches with 1 hr of ethanol then: 10 mins hexane (M9), 1 hr hexane (M10), and 4 hrs hexane (M11) at different pressures	161
Figure 5.26	Ideal selectivity of CO ₂ /N ₂ for membranes dried using vacuum drying (M8) and solvent-exchange approaches with 1 hr of ethanol then: 10 mins hexane (M9), 1 hr hexane (M10), and 4 hrs hexane (M11) at different pressures	163
Figure 5.27	Single gas permeances (GPU) of (a) CO ₂ , (b) N ₂ gas for membranes dried using vacuum drying (M8) and dried with solvent-exchange approaches with: 10 mins ethanol (M12), 1 hr ethanol, (M10), and 4 hrs ethanol (M13) then 1 hr of hexane at different pressures	166
Figure 5.28	Ideal selectivity of CO ₂ /N ₂ for membranes dried using vacuum drying (M8) and with solvent-exchange approaches with: 10 mins ethanol (M12), 1 hr ethanol, (M10), and 4 hrs ethanol (M13) then 1 hr of hexane at different pressures	167

Figure 5.29	CO ₂ kinetic uptake curves for membranes dried using vacuum drying (M8) and solvent-exchange approaches with 1 hr of ethanol then: 10 mins hexane (M9), 1 hr hexane (M10), and 4 hrs hexane (M11)	169
Figure 5.30	CO ₂ solubility coefficient for membranes dried using vacuum drying (M8) and solvent-exchange approaches with 1 hr of ethanol then: 10 mins hexane (M9), 1 hr hexane (M10), and 4 hrs hexane (M11)	172
Figure 5.31	CO ₂ kinetic uptake curves for membranes dried using vacuum drying (M8) and with solvent-exchange approaches with: 10 mins ethanol (M12), 1 hr ethanol, (M10), and 4 hrs ethanol (M13) then 1 hr of hexane	174
Figure 5.32	CO ₂ solubility coefficient for membranes dried using vacuum drying (M8) and with solvent-exchange approaches with: 10 mins ethanol (M12), 1 hr ethanol, (M10), and 4 hrs ethanol (M13) then 1 hr of hexane	176
Figure 5.33	CO ₂ permeance of binary CO ₂ /N ₂ gas mixture through mixed matrix membrane of 0.1 wt% of MWCNTs-F1 and 4 hrs ethanol followed by 1 hr n-hexane exchange drying as a function of CO ₂ feed composition at 1 bar	178
Figure 5.34	Composition selectivity of binary CO ₂ /N ₂ gas mixture through mixed matrix membrane of 0.1 wt% of MWCNTs-F1 and 4 hrs ethanol followed by 1 hr n-hexane exchange drying as a function of CO ₂ feed composition at 1 bar	179
Figure 5.35	Schematic representing the effects of binary CO ₂ /N ₂ gas mixture at (a) low CO ₂ feed composition, (b) equivolume of CO ₂ /N ₂ feed composition, and (c) high CO ₂ feed composition	180
Figure C.1	Calibration curve for (a) CO ₂ and (b) N ₂	212
Figure D.1	Chromatogram of CO ₂ /N ₂ binary gas mixture at (a) permeate and (b) retentate streams	214

LIST OF PLATES

		Page
Plate 4.1	Photograph of MWCNTs at different β -CD concentration of (a) 30 wt% (MWCNTs-F1), (b) 20 wt% (MWCNTs-F2), and (c) 10 wt% (MWCNTs-F3)	69
Plate 4.2	Photograph of heating mantle	71
Plate 4.3	The photograph of the gas permeation and separation test rig	89
Plate 4.4	Photograph of the gas permeation cell	90
Plate 5.1	TEM micrographs of MWCNTs-P	97
Plate 5.2	TEM micrographs of MWCNTs at different β -CD concentration of (a,b) 30 wt% (MWCNTs-F1), (c,d) 20 wt% (MWCNTs-F2), and (e,f) 10 wt% (MWCNTs-F3)	104
Plate 5.3	TEM micrographs of MWCNTs at different non-aqueous media of (a,b) ethanol (MWCNTs-F1), (c,d) acetic acid (MWCNTs-F4), and (e,f) water (MWCNTs-F5)	113
Plate 5.4	TEM micrographs of MWCNTs-F1 (a,b) without washing, and (c,d) with three repeated washing steps	117
Plate 5.5	FESEM cross sectional morphologies of membrane with casting thickness of (a) 300 μm (M2), (b) 250 μm (M3), and (c) 150 μm (M4)	120
Plate 5.6	FESEM micrographs of membrane surface (left) and cross section (right) structure fabricated at polymer concentration of (a,b) 7 wt% (M1), (c,d) 10 wt% (M3), (e,f) 15 wt% (M5), and (h,i) 17 wt% (M6) with casting thickness of 250 μm	125
Plate 5.7	FESEM cross sectional morphologies for membrane with (a) conventional vacuum drying method (M3) and (b) solvent-exchange drying method of 4 hrs ethanol followed by 1 hr n-hexane (M7)	130
Plate 5.8	FESEM morphologies of surface and cross section of (a-b) as spun CA membrane (M7) and (c-d) mixed matrix membrane with MWCNTs-P (MMM-0.1P)	137

Plate 5.9	FESEM morphologies of mixed matrix membrane with MWCNTs-F1 (MMM-0.1F) (a) surface and (b) cross section	138
Plate 5.10	FESEM morphologies of surface and cross section of mixed matrix membrane at different MWCNTs-F1 loadings of (a) 0.05 wt%, (b) 0.1 wt%, (c) 0.2wt%, and (d) 0.3 wt%	146
Plate 5.11	FESEM cross section micrograph of membrane with (a) vacuum drying (M8) and solvent-exchange approaches with 1 h of ethanol then: (b) 10 mins hexane (M9), (c) 1 hr hexane (M10), and (d) 4 hrs hexane (M11)	159
Plate 5.12	FESEM cross section micrograph of membrane that exchanged with: (a) 10 mins (M12), (b) 1 hr (M10), and (c) 4 hrs (M13) of ethanol; then exchanged with 1 hr of hexane	164

LIST OF ABBREVIATIONS

[BMIM]SCN	1-butyl-3-methylimidazolium thiocyanate
2-HB- β -CD	2-hydroxybutyl-beta-cyclodextrins
AFM	Atomic force microscopy
AgX	Commercial catalyst
APDEMS	(3-aminopropyl)-diethoxymethyl silane
BET	Brunauer-Emmett-Teller
BJH	Barrett-Joyner-Halenda
BPPO	Brominated poly(2,6-diphenyl-1,4-phenylene oxide)
BWC	Bounded water content of the membrane
CA	Cellulose acetate
CCS	Carbon capture and storage system
CD	Cyclodextrins
CH ₃ COOH	Acetic acid
CH ₄	Methane
CMS	Carbon molecular sieves
CNTs	Carbon nanotubes
CO ₂	Carbon dioxide
D band	Defect band
DLS	Dynamic light scattering
DMAC	Dimethylacetamide
DMF	Dimethylformamide
FESEM	Field emission scanning electron microscopy
FTIR	Fourier transform infrared spectroscopy

G band	Graphite band
GC	Gas chromatography
GHSs	Greenhouse gases
Gt	Giga tons
H ₂ O	Water vapor
H ₂ S	Hydrogen sulfide
HFCs	Hydrofluorocarbons
I _D	Intensity of D band
I _G	Intensity of G band
MMM	Mixed matrix membrane
MMMs	Mixed matrix membranes
MOFs	Metal organic frameworks
MWCNTs	Multi walled-carbon nanotubes
MWCNTs-F	Functionalized-multi walled-carbon nanotubes
MWCNTs-P	Pristine-multi walled-carbon nanotubes
N ₂	Nitrogen
N ₂ O	Nitrous oxide
NaX	Commercial catalyst contains a binder consisting of Al and/or Si based compound
NH ₃	Ammonia
NMP	N-methylpyrrolidone
O ₂	Oxygen
O ₃	Ozone
PDMS	Polychmethyl siloxane
PEG	Polyethyleneglycol

PES	Polyethersulfone
PFCs	Perfluorocarbons
PI	Polyimide
R _a	Mean roughness
R _{RMS}	Root mean square
SF ₆	Sulfur hexafluoride
STP	Standard temperature and pressure
SWCNTs	Single-walled carbon nanotubes
TCD	Thermal conduction detector
TEM	Transition electron microscopy
TGA	Thermo gravimetric analysis
XRD	X-ray diffraction

LIST OF SYMBOLS

A_m	Effective membrane area
C_∞	Concentration of the sample after 150 min
C_o	Initial concentration
C_t	Concentration at time
D	Diffusivity coefficient
dp	average pore diameter
I	Intensity
I_o	Background intensity
l	Dense skin layer thickness of the membrane
M_A	Molecular weight of gas component
M_t/M_∞	CO ₂ sorption uptake
N_i	Flux of the gas sample of component i
p	Pressure
Δp	Pressure difference across the membrane
P	Permeability
P/l	Permeance
S	Solubility coefficient
t	Time
T	Temperature

Greek letters

α Selectivity

μ Viscosity

β Beta

γ Gamma

Subscript

i,j Component of CO₂ and N₂

m membrane

t time

Superscript

Comp Composition

**MEMBRAN MATRIKS BERCAMPUR TIUB NANO KARBON DINDING
BERLAPIS YANG BERKEBERANGKAPAN/SELULOSA ASETAT BAGI
PEMISAHAN CO₂/N₂**

ABSTRAK

Karbon dioksida (CO₂) adalah salah satu penyumbang utama kepada kesan rumah hijau kepada bumi, yang kuantitinya kian meningkat sejak revolusi industri. Salah satu cara untuk mengurangkan pelepasan CO₂ adalah dengan menghasilkan membran yang cekap dan mantap yang mampu menapis mengikut kememilihan CO₂. Antara bahan dan sifat membran yang pelbagai, membran matriks bercampur (MMB) merupakan satu pendekatan alternatif yang menggabungkan sifat-sifat pemisahan zarah-zarah bukan organik dengan keupayaan proses polimer ke dalam satu sistem. Dalam kajian ini, MMB dihasilkan daripada polimer selulosa acetate (CA) dan tiub nano karbon dinding berlapis yang berkeberangkapan (MWCNTs-F) menerusi songsangan fasa basah. Beta-cyclodextrins (β-CD) telah digunakan untuk berkeberangkapan dinding sisi MWCNTs untuk penyebaran yang lebih baik dalam matriks polimer CA tanpa mengubah struktur asli dan sifatnya. Darjah berkeberangkapan telah ditingkatkan dengan meningkatkan nisbah β-CD di bawah penggunaan media air dengan kadar lebih rendah pelarut kecutuban 5.2. Lapisan membran yang padat dan nipis tanpa kecacatan dengan ketebalan 250 μm, kepekatan polimer 10 wt% dan dikeringkan dengan menggunakan kaedah pengeringan telah berjaya disintesis melalui pertukaran pelarut. Bila berkeberangkapan MWCNTs telah digabungkan ke dalam formula optimum CA polimer matriks, ukuran gas penelapan menunjukkan prestasi cemerlang MMB dari segi kebolehtelapan dan darjah kememilihan pada 0.1 wt% amoun MWCNTs-F1. Prestasi yang tinggi ini adalah

disebabkan oleh penyebaran seragam antara MWCNTs-F1 dan matriks CA yang meningkatkan isipadu bebas yang mencukupi antara rantai an polimer dan menambahkan antaramuka polimer/nanofiller, seperti yang disahkan oleh keputusan pembiasan sinar-x. Selain itu, keputusan pemisahan telah menyokong keberkesanan teknik pertukaran-pelarut yang baru dicadangkan, di mana MMB dengan 4 jam etanol diikuti oleh 1 jam n-heksana menunjukkan peningkatan dalam kekuatan mekanikal membran dan menunjukkan prestasi pemisahan CO₂/N₂ yang lebih baik pada 40.17. Pengambilan serapan CO₂, pekali resapan, dan pekali kebolehlarutan juga diambil kira dalam kajian ini. Keputusan menunjukkan bahawa pekali kebolehlarutan mempunyai pengaruh langsung terhadap kebolehtelapan CO₂ dengan nilai tertinggi $198.352 \times 10^{11} \text{ cm}^3(\text{STP}) / \text{cm}^4 \cdot \text{cmHg}$ untuk sampel membran M13 (4 jam etanol kemudian 1 jam n-heksana). MMB optimum ini telah digunakan lagi untuk kajian kebolehtelapan gas perduaan dan darjah kememilihan CO₂/N₂. Komposisi suapan dari CO₂/N₂ 50:50 vol% menunjukkan darjah kememilihan CO₂/N₂ yang tertinggi iaitu 17.36 ± 1.16 . Sepanjang kajian pembentukan membran, prestasi pemisahan gas telah dianalisa melalui korelasi pelbagai struktur membran dan sifat-sifat fizikal yang membolehkan pemisahan CO₂ secara khusus.

**FUNCTIONALIZED MULTI-WALLED CARBON
NANOTUBE/CELLULOSE ACETATE MIXED MATRIX MEMBRANE FOR
CO₂/N₂ SEPARATION**

ABSTRACT

Carbon dioxide (CO₂), as one of the major atmospheric contributors to the Earth's greenhouse effect has been rising extensively since the industrial revolution. One promising means of lowering the emission of CO₂ is to develop highly efficient and robust membranes that are capable of selective CO₂. Within the wide range of materials and properties for membranes, the mixed matrix membrane (MMM) starts to emerge as an alternative approach, where it combines the separation properties of inorganic particles with the process ability of polymers into one system. In this study, the MMM was synthesized from the cellulose acetate (CA) polymer and the functionalized multi-walled carbon nanotubes (MWCNTs-F) through wet-phase inversion. Beta-cyclodextrins (β -CD) was used to functionalize the sidewalls of MWCNTs for better dispersion in CA polymer matrix without changing their pristine structure and properties. The degree of functionalization was increased by increasing the β -CD ratios under the usage of a non-aqueous media with lower solvent polarity of 5.2. A defect-free, thin, dense skin thickness of membrane was successfully synthesized at casting thickness of 250 μ m, polymer concentration of 10 wt%, and dried using the solvent-exchange drying method. When the functionalized MWCNTs were incorporated into the optimum formulation of CA polymer matrix, the gas permeation measurements showed excellent MMM performances in terms of permeance and selectivity at 0.1 wt% loadings of MWCNTs-F1. This superior

performance was due to the homogeneous dispersion between MWCNTs-F1 and the CA matrix, which increased the sufficient free volumes between the polymer chains and enlarged the polymer/nanofiller interface, as confirmed by the X-ray diffraction results. Furthermore, the separation results have supported the effectiveness of the newly proposed solvent-exchange technique, where the MMM with 4 hrs ethanol followed by 1 hr n-hexane showed improvement in the membrane's mechanical strength and performed with a better CO₂/N₂ separation performance at 40.17. The CO₂ sorption uptake, diffusion coefficient, and solubility coefficient were also considered in this work. The results indicated that the solubility coefficient had a direct influence on the CO₂ permeance with a highest value of $198.352 \times 10^{11} \text{ cm}^3(\text{STP})/\text{cm}^4 \cdot \text{cmHg}$ for the membrane sample M13 (4 hrs ethanol then 1hr n-hexane). This optimum MMM was further used to study the binary gas permeance and CO₂/N₂ selectivity. The feed composition of CO₂/N₂ for 50:50 vol% showed the highest CO₂/N₂ composition selectivity at 17.36 ± 1.16 . Throughout the membrane formation study, the potential gas separation performance was interpreted in correlation to various membrane structures and its physical properties, which enabled the separation of CO₂ in a specific manner.

CHAPTER ONE

INTRODUCTION

1.1 Global Issues of Carbon Dioxide as a Greenhouse Gas

One of the most challenging issues that need to be addressed in the world today is the control of anthropogenic emissions of greenhouse gases (GHGs). Carbon dioxide (CO₂) is the largest contributor amongst these GHGs. Due to its high amount present in the atmosphere, CO₂ contributes 60 % of the global warming effects (Yamasaki, 2003; He and Hägg, 2011).

The development of low-emission fossil fuel technologies combined with the carbon capture and storage system (CCS) has been proposed to reduce the adversities of climate change caused by the emission of GHGs particularly CO₂. The CCS types are pre-combustion, oxy-combustion capture, post-combustion and other industrial separation techniques (Zhao *et al.*, 2008). In pre-combustion, the CO₂ is captured prior to combustion. Meanwhile, in oxy-combustion capture, the fossil fuel is burnt using oxygen enriched air. In this case, a higher concentration of CO₂ is generated facilitating the efficient removal of CO₂ (Reijerkerk *et al.*, 2011).

On the other hand, in the case of post-combustion capture, the CO₂ is captured after the fossil fuel has been burned with normal air (Reijerkerk *et al.*, 2011). The post-combustion process captures CO₂ from flue gases produced by the combustion of fossil fuels and biomass. Power plants emit more than one-third of all CO₂ emissions worldwide (Zhao *et al.*, 2008). Typically, the flue gas contains mainly

CO₂ (4 to 30 %) and nitrogen (N₂, ~86 to 53 %). The other compounds are oxygen (O₂, ~5 %) and water vapor (H₂O, ~5 to 12 %) (Favre, 2007).

Gas separation in this process can be accomplished by either the chemical solvent technology or membrane technology. In spite of its popularity, the chemical solvent technology has certain limitations such as expensive operational costs, high heat reaction with CO₂, and corrosive nature of some solvents (Diwekar and Shastri, 2011). In contrast, gas separation using membrane technology provides good benefits such as energy efficiency, utilization of non-toxic chemicals, and simple operating procedures that make it extremely attractive for CO₂ capture (Bernardo and Clarizia, 2011). In terms of energy requirements, membrane technology is comparable to the adsorption of flue gases containing 20 % or more of CO₂ (Favre, 2007). Numerous studies have shown the economic benefits of membrane based separation systems with a high concentration of CO₂ (Baker and Lokhandwala, 2008).

1.2 Membrane Gas Separation

The improvement of CO₂ separation efficiency from flue gases to reduce the total energy cost of sequestration technologies in coal-fired power plants has been identified as a high-priority research area. In the past three decades, membranes have attracted the attention of chemists and engineers due to their unique separation principles (i.e., selective transport and efficient separation compared to other unit operations) (Saxena *et al.*, 2009).

In fact, the polymeric membranes also have several limitations for gas separation such as low selectivity, high temperature instability, swelling and decomposition in organic solvents (Shelekhin *et al.*, 1992). These limitations have led to the development of alternative membrane materials (inorganic membranes) that are synthesized from metal, ceramics or pyrolyzed carbon. Although the properties of some inorganic materials are well above the trade-off curve for polymers, it is challenging to duplicate the enlarged-scale modules containing thousands of square meters of membrane areas due to the high capital costs. In addition, the brittleness and low surface-to-ratio volume of inorganic membranes are also the challenges to fully optimize their applications for gas separation industries (Goh *et al.*, 2011). In this regard, mixed matrix membrane (MMM) is proposed in the current study.

1.3 Mixed Matrix Membrane (MMM)

The improvement of membrane separation properties can be achieved by the development of MMMs. The MMMs are recently getting more attention as an attractive candidate for membrane-based separation (Ismail *et al.*, 2009), where it has a bright future as an alternative to conventional polymeric and inorganic membranes. The incorporation of inorganic components such as zeolite (Jiang *et al.*, 2006b; Funk and Lloyd, 2008; Gorgojo *et al.*, 2008), carbon molecular sieves (CMS) (Rafizah and Ismail, 2008; Itta *et al.*, 2010; Weng *et al.*, 2010), and carbon nanotubes (CNTs) (Kim *et al.*, 2007; Ismail *et al.*, 2009; Qiu *et al.*, 2009; Aroon *et al.*, 2010b; Wu *et al.*, 2010) into the polymer matrix enable MMMs to have the potential to achieve higher selectivity and/or permeability relative to existing polymeric membranes

(Moore *et al.*, 2004; Jain *et al.*, 2008; Ismail *et al.*, 2009; Itta *et al.*, 2010). This phenomenon is illustrated in Figure 1.1.

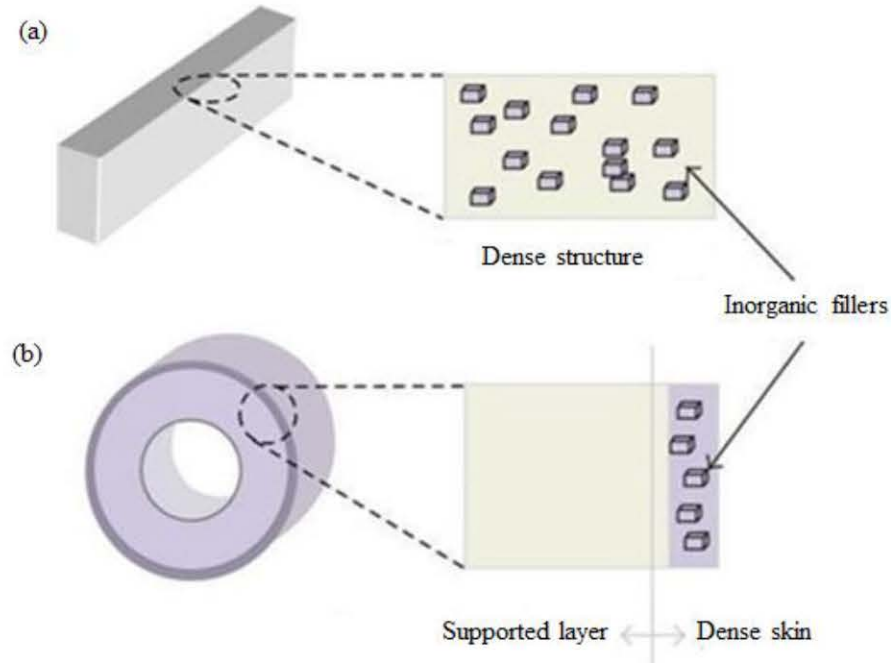


Figure 1.1: MMMs in configuration: (a) symmetric flat dense, and (b) Asymmetric hollow fiber (Goh *et al.*, 2011)

1.4 Importance of MMM

MMMs have advantages such as excellent gas separation performance (Zimmerman *et al.*, 1997), enhanced mechanical properties of polymeric materials (Cong *et al.*, 2007b) and the creation of a thin selective layer (Mahajan and Koros, 2000). The separation properties of inorganic fillers, such as zeolite, CMS, and silica nanoparticles (Moore *et al.*, 2003; Itta *et al.*, 2010; Ahn *et al.*, 2011; Dorosti *et al.*, 2011; Shen and Lua, 2012), can be used to enhance the selectivity for a given gas mixture by increasing the sorption of the desired gas component within the MMM (Ismail *et al.*, 2011). Although the sieving characteristics of zeolite and CMS are attractive, their sizes and aspect ratios are less favorable for the production of asymmetric membranes with thin selective layers (Goh *et al.*, 2011). Thus,

addressing the challenges posed by the MMM which are focused on utilizing promising alternative materials, such as CNTs, clay, and metal organic framework, to solve the existing problems and improve the membrane separation performance (Goh *et al.*, 2011). Among all choices, CNTs have shown to be a very promising filler in the polymeric matrix that is suited for membrane based separation (Bikiaris *et al.*, 2008; Ismail *et al.*, 2011). This is due to their unique properties such as high aspect ratio, high surface area, frictionless surface, and strong mechanical properties (Ismail *et al.*, 2009). In short, MMMs possess promising properties compared to the polymeric and inorganic membranes. These are briefly summarized in Table 1.1 (Ismail *et al.*, 2009).

Table 1.1: Comparison of the properties for polymeric, inorganic and MMM (Ismail *et al.*, 2009)

Properties	Polymeric Membrane	Inorganic Membrane	MMM
i. Cost	economical to fabricate	high fabrication cost	moderate
ii. Chemical and thermal stability	moderate	high	high
iii. Mechanical strength	good	poor	excellent
iv. Compatibility to solvent	limited	wide range	limited
v. Swelling	frequently occurs	free of swelling	free of swelling
vi. Separation performance	moderate	moderate	exceed Robeson upper boundary
vii. Handling	robust	brittle	robust

1.5 Problem Statement

The recovery of carbon dioxide from large emission sources is a formidable technological and scientific challenge which has received considerable attention for several years. A great number of engineering studies has been dedicated to the achievement of this goal in order to restrict greenhouse gases emissions, which remains the number one challenge of global warming scenario (Favre, 2007). In fact, the CO₂ concentration in the flue gas typically, 3-5 mol % in gas plants and 13-15 mol% in coal plants, in turn, the cost of capture would be significant (Zhao *et al.*, 2008).

Gas separation through polymeric membranes offer several advantages compared to conventional processes, such as low capital investment, low energy consumption, environmental benignancy, ease of operation, and versatility. This separation technique has been shown to be a potential alternative to traditional processes (Koros and Mahajan, 2000; Basu *et al.*, 2011), particularly to amine-based wet scrubbing (Basu *et al.*, 2011). The fabrication of appropriate membranes for gas separation is aimed at improving gas permeability and selectivity. However, it remains as one of the major challenges for researchers (Weng *et al.*, 2009; Zhang *et al.*, 2010). To achieve excellent gas separation performance, the synthesized membranes should have a thin, dense skin layer that is supported by a thick porous sub-layer (Qin and Chung, 2004; Rahman, 2004), which provides mechanical resistance to the skin and low resistance to gas transport (Ferreira Júnior *et al.*, 2011). Furthermore, the dense selective layer must be virtually defect-free to assure that permeation is exclusively controlled by a solution/diffusion mechanism (Chung *et al.*, 2000).

Recently, several attempts have been made to increase membrane performance in gas separations using MMMs (Zimmerman *et al.*, 1997). As discussed earlier, MMMs consist of dispersed phase of inorganic particles, such as zeolite, carbon molecular sieves, or CNTs, embedded in the continuous phase of a polymeric matrix (Ismail *et al.*, 2009; Aroon *et al.*, 2010a). The MMMs overcome the individual deficiencies of inorganic particles and polymers to achieve a high CO₂ separation performance (Scholes *et al.*, 2008). However, the poor interfacial compatibility between the inorganic fillers and the polymer leads to the formation of unselective channels within the membrane (Mahajan and Koros, 2000). Thus, there is a need to enhance the compatibility between the inorganic fillers and the polymeric components within MMMs. To date, no reports have addressed the separation performance of CO₂/N₂ by MMM comprising of CA polymer matrix and CNTs. It is believed that this hybrid MMM (CA-CNTs) is able to attract attentions by combining the advantages of both the CA polymer (i.e., high CO₂ solubility) and MWCNTs (i.e., enhanced physical and mechanical properties) for gas separation applications.

CNTs have been chosen as inorganic filler in the present study due to their chemically inert properties and inability to disperse in typical organic solvents, which is still uncertain (Qiu *et al.*, 2009; Sanip *et al.*, 2009). Therefore, numerous efforts have been focused on functionalizing and modifying CNTs to improve their dispersion ability (Qiu *et al.*, 2009; Sanip *et al.*, 2009). A proper CNT's functionalization is difficult because of the inherently inert nature of carbon atoms. The CNTs have two distinct regions, end tips and sidewalls, each with different chemical reactivity. The pentagons at the end tips of CNTs are dynamically more reactive than the hexagons on the sidewalls. Thus, sidewall functionalization within

the regular graphene framework cannot be easily accomplished (Kim, 2011b). Considering this drawback, the non-covalent functionalization method is suggested in the present study. As far as it is known, there have been no studies presenting any concrete evidence on the effect of the solvent polarity as a medium on the understanding of the highly functionalized MWCNTs. Thus, it is important to investigate this effect through an environmentally friendly method without changing their pristine structures and properties of CNTs.

Moreover, as for gas separation, the synthesized membrane must be dried before use (Kailash C., 2007). The challenge of the current work is to dry the newly synthesized MMM without any structure rapture. In fact, the water contained within the CA membrane is difficult to remove because of its asymmetric structure (Kailash C., 2007). Therefore, a lot of effort was needed to focus on improving the drying methods of CA membrane for gas separation (Jie *et al.*, 2005). Riley *et al.* (1964) reported the replacement of water in a wet CA membrane with carbon tetrachloride by liquid extraction to obtain a dry CA membrane. However, this method is time consuming. Therefore, there is an urgent need to find an easy and effective method to dry the synthesized MMM, in order to maintain the MMM structure and to attain higher CO₂ permeance and CO₂/N₂ selectivity.

1.6 Research Objectives

The aim of the present work is to develop a defect-free MMM with a thin and dense-skin layer for high separation performance towards CO₂/N₂. This can be achieved if MWCNTs are dispersed and attached well within the polymer matrix. In this regard, the objectives of this research are:

- 1) Study the influence of β -CD concentration ratio (the dispersant) and the effect of non-aqueous media on the functionalization degree, structures and properties of functionalized MWCNTs
- 2) To synthesize and optimize the final CA membrane structure and its properties such as dense structure, surface roughness, and gas separation performance.
- 3) To study the correlation between MWCNTs and CA in developing a defect-free MMM with a thin and dense-skin layer for high separation performance toward CO_2/N_2 .
- 4) To develop a dry MMM and overcome the problems of membrane structure rupture to improve CO_2/N_2 separation performance.
- 5) To study the kinetic sorption of the MMMs dried under conventional vacuum drying and solvent-exchange drying methods.

1.7 Scope of Study

The influence of β -CD concentration ratio from 10 wt% to 30 wt% and the effect of non-aqueous media i.e., ethanol, acetic acid, and water on the functionalization degree, structures and properties of functionalized MWCNTs (MWCNTs-F) will be studied. The MWCNTs-Pristine (MWCNTs-P) and MWCNTs-F samples will be characterized using Fourier transform infrared spectroscopy (FTIR), Raman spectroscopy, transition electron microscopy (TEM), dynamic light scattering (DLS), thermo gravimetric analysis (TGA), and X-ray diffraction (XRD) to confirm the effectiveness of the resulting functionalization.

In this study, the properties of a CA membrane, in terms of membrane casting thickness (150 μm to 300 μm), CA polymer concentration (7 wt% to 17 wt%), and drying methods (conventional vacuum drying and solvent-exchange drying), will be evaluated. The membranes will be characterized using field emission scanning electron microscopy (FESEM) and Atomic force microscopy (AFM). In terms of membrane performance, CO_2 permeance and CO_2/N_2 separation were determined. The optimal CA membrane obtained from the three factors will be further used to synthesize the MMM.

In the MMM synthesis, MWCNTs-F were incorporated into the CA polymer matrix. The effect of various concentration loadings of MWCNTs-F in CA polymers was evaluated. Furthermore, physical and separation properties of CA-MWCNTs-F and CA-MWCNTs-P were then compared by measuring the permeance and selectivity towards the separation of CO_2 from CO_2/N_2 .

It is essential to find the optimum drying method as well as the proper drying time for the newly synthesized MMM. Thus, both conventional vacuum drying and ethanol-hexane drying at different exchange time of solvents (hexane and ethanol) will be compared in terms of the membrane morphologies and gas separation performance. The results were confirmed by using FESEM and bounded water content. With regards to the membrane separation performance, the CO_2/N_2 permeance and selectivity were carried out. In addition, the kinetic sorption of the synthesized MMMs dried using ethanol-hexane drying methods at different exchange times of solvents and the controlled MMM, dried under the conventional vacuum drying method, was further studied. The CO_2 sorption uptake, CO_2 diffusion

coefficients, and CO₂ solubility coefficients were determined in order to identify the driving force for the CO₂ transport through the prepared MMMs.

Lastly, the optimum synthesized MMM was tested under CO₂/N₂ binary gas mixture to investigate whether this MMM would have the opportunity to meet the industrial requirement for post-combustion CO₂ separation under flue gas conditions. In this regard, the CO₂ feed composition of 20 vol%, 50 vol%, and 80 vol% were utilized to evaluate the permeation and separation performances.

1.8 Organization of Thesis

This thesis is outlined in six chapters. Each chapter is summarized and addressed as below:

In Chapter one, a brief introduction about the global issues of CO₂ as a greenhouse gases was addressed and focused on the technologies to separate the CO₂. Moreover, the overview of MMM definition and properties were also addressed in this chapter. All current issues, problem statements and research objectives were also outlined in the later sections. This was followed by the scope of the present study and organization of the thesis.

In Chapter two, a review about the post combustion CO₂ capture methods to separate the CO₂ was presented. The application of MMM for gas separation was outlined. Subsequently, the phenomenon to develop the MMM was reviewed. Besides, the alternatives and challenges to embed the inorganic fillers were also highlighted in this chapter. As for membrane synthesis, the effecting parameters in

fabrication of CA membrane were discussed. In the last part of this chapter, the fundamental transport mechanisms in gas separation membrane were explored.

In Chapter three, the kinetic sorption model for gas permeation was discussed. The assumptions for the gas separation were presented. Then, the mathematical derivation of the kinetic sorption for the transport of CO₂ in the MMM was explained in detail. Lastly, the gas permeation model for solution-diffusion mechanism was also derived.

Chapter four covers the detail of the materials and experimental procedures. The CNTs functionalization, synthesis of CA membrane, and the development of MMM with CA polymer and MWCNTs were elucidated. Clear descriptions for the various characterization techniques were also reported. This chapter presents the operating procedure of the test rig to determine the CO₂/N₂ permeance and selectivity performance.

Chapter five presents the results of the experiments and their related explanation according to the objectives. Investigations about the variables to functionalize the CNTs with environmentally friendly soft-cutting method were discussed. In the second section, the effects of CA membrane fabrication parameters on the morphology, surface microstructure, and gas separation performance were studied. In order to synthesize the MMM, the incorporation of MWCNTs into CA polymer matrix was investigated in the third section. Moreover, the effects of MWCNTs loading on the MMM structure and CO₂/N₂ separation were also evaluated. This chapter also focused on finding the proper drying method to dry off

the newly synthesized MMM. Both conventional vacuum drying and solvent-exchange drying methods at different exchange time of solvents were discussed in the chapter. Besides, the kinetic sorption was also studied to determine the CO₂ sorption uptake, diffusion coefficients, and solubility coefficient.

In the last chapter (Chapter six), the findings of the present study were concluded point by point according to the research objectives. In addition, some recommendations for future development and application of MMM from CNTs and CA polymer matrix were also proposed in this chapter.

CHAPTER TWO

LITERATURE REVIEW

2.1 The Global Issues of Greenhouse Gas

The earth's atmosphere contains trace constituents absorbing radiation in the thermal radiation range of the plant. Therefore, the energy absorbed into the atmosphere in this way, is being radiated partly back to increase the temperature of the surface. The major trace constituents warming the planet are carbon dioxide (CO₂), methane (CH₄), nitrous oxide (N₂O), sulfur hexafluoride (SF₆), hydrofluorocarbons (HFCs), and perfluorocarbons (PFCs). These trace constituents are usually known as greenhouse gases (GHGs) (Trexler and Kosloff, 1998; Haszpra, 2011).

The atmospheric concentration of the different GHGs has significantly increased since 1950 because of the increased in human activity. Based on scientific reports, the concentration of CO₂ has increased by about 30% during the last 200 years. Meanwhile, the concentration of CH₄ has increased to double and the concentration of N₂O has increased to nearly 15% (Shafeen and Carter, 2010).

2.1.1 The Effects of Greenhouse Gas

The changes in the atmospheric amount of GHGs have resulted in the redistribution of energy in the atmosphere-surface system. Consequently, this leads to changes in the earth's surface temperature that will eventually change the global climate. The relation between the concentration of GHGs and the extent of the climate changes is extremely complex because of the increment in the atmospheric

GHGs amount and the partly poor knowledge of feedback and interaction behavior (Haszpra, 2011).

The increased concentrations of key GHGs are a direct consequence of human activities. Since anthropogenic GHGs accumulate in the atmosphere, they produce net warming by strengthening the natural “greenhouse effect”. Various reports from assumed that the concentrations of CO₂ will be ramping up from current 280 ppmv to as high as 970 ppmv in the year 2100. As a consequence, the globally averaged surface temperature is projected to rise by 1.4–5.8 °C over the period 1990–2100, with a warming rate likely to be unprecedented during at least the last 10 000 years (Quadrelli and Peterson, 2007).

One of the greatest examples in explaining the climate change phenomenon is in relation to the oil-bearing basins. In these plants, half of the associated gas is usually burnt in flares. Consequently, CO₂, N₂O, hydrocarbons and soot are released to the atmosphere. In fact, the release of CO₂ contributes to the greenhouse effect (Lombardi *et al.*, 2006). For these reasons and with the increased international interest and cooperation aimed at policy-oriented solutions to solve the problem of climate change, the GHGs assessment emitted to and/or removed from the atmosphere has been highly emphasized in both the political and scientific agendas internationally (Lieberman *et al.*, 2010).

2.1.2 The Removal of CO₂

In general, the most important cause of climate change is the increasing atmospheric concentration of CO₂. This is mainly because of the dependence on fossil fuels by the world's economy (Reijerkerk *et al.*, 2011). Further, CO₂ is emitted from the sweetening of natural gas, the production of synthesis gas, and certain chemical plants (Huang *et al.*, 2008). In fact, more than half of the global emission of CO₂ (55%) are produced by power plants and heavy industries such as petroleum, cement, and steel manufactures (Hussain and Hägg, 2010).

Since the industrial revolution, CO₂ emissions from fuel combustion dramatically increased to 26.6 Gt CO₂ per year. In 2004, CO₂ emissions from fossil fuel combustion were roughly twice compared to those of 30 years before. The world energy supply is projected to rise by 52% between 2004 and 2030. With fossil fuels remaining at 81% of the total primary energy supply, CO₂ emissions are consequently expected to continue their growth unabated, reaching 40.4 Gt CO₂ by 2030. Besides, land use change and forestry account for a large majority of total CO₂ emissions as a result of heavy deforestation, which is an issue for both hydropower and biomass production (Quadrelli and Peterson, 2007).

Statistically, over the past several hundred years, the concentration of atmospheric CO₂ has steadily increased from the pre-industrial level of 280 ppm to over 370 ppm (Thomas and Benson, 2005). Currently, the concentration of atmospheric CO₂ has increased to 390.5 ppm (Humlum *et al.*, 2013). This increment is mainly ascribed to the burning of coal, oil, and natural gas for electrical generation, transportation, industrial and domestic usage. At today's emission rates,

globally, over 20 billion tons of CO₂ have been emitted into the atmosphere (Thomas and Benson, 2005). Furthermore, based on the report from the International Energy Outlook 2010 (IEO2010), the world energy-related CO₂ emissions will increase from 29.7 billion metric tons in 2007 to the estimated 33.8 billion metric tons in 2020 and 42.4 billion metric tons in 2035 (International Energy Outlook, 2010). Thus, one of the major issues haunting environmentalists in both the developed and developing countries is the control of anthropogenic CO₂ emissions (Aaron and Tsouris, 2005).

In order to reduce the total emission of CO₂, there are three common practices that are widely applied (1) reduce the energy consumption (2) minimize fossil fuels usage or (3) CO₂ capture and storage (CCS) (He and Hägg, 2011). The first two choices are required for efficient usage of energy and the switch to the applications of non-fossil fuels such as hydrogen or renewable energy. Meanwhile, the CCS is about the development of new efficient technologies for CO₂ separation (He and Hägg, 2011).

The practical applications of CO₂ capture are at the largest point sources of CO₂ such as electricity generating plants (coal-fired and natural gas-fired), natural gas upgrading plants, oil refineries, iron/steel plants, and lime/cement plants (Thomas and Benson, 2005). The fossil fuel power plants have emitted a large quantity of CO₂, at roughly 40% of CO₂ total emissions especially for the coal-fired plants. Until today, CCS is still considered as the most applicable option to reduce the emission of CO₂ from the industries (He and Hägg, 2011).

There are many dedicated researchers trying to enhance the current technologies or develop new methods for CO₂ capture. In general, the separation processes of CO₂ can be classified as the chemical and physical absorption, membranes, adsorption and cryogenic fractionation (Zhao *et al.*, 2008; He and Hägg, 2011). The selection of suitable methods will be mainly dependent on the characteristics of the treated gas as well as the process conditions (He and Hägg, 2011). In fact, the chemical absorption method and membrane technology are the most practical options for CO₂ capture in the post-combustion process (Zhao *et al.*, 2008). Hence, both techniques will be discussed in detail in the following section.

2.1.2 (a) Chemical Absorption Method

The ammonia scrubbing process based on chemical absorption using amine based solvent plays a dominant role in CO₂ capture (Zhao *et al.*, 2008). Currently, many plants have been practicing this technology in their full-scale demonstration of power plants for CO₂ separation. These include RWE 500MWe coal-fired power plant (PCC) in Tilbury, UK; Statoil/Shell 860MWe natural gas power plant (NGCC) in Tjeldbergodden, Norway; and Statoil/Dong 280MWe natural gas power plant (NGCC) in Mongstad, Norway (Zhao *et al.*, 2008).

In Figure 2.1, the process flow chart for amine separation is depicted. Basically, in this process, the flue gas was contacted with the amine based solution in an absorber. Then, the amine based solvent absorbs the CO₂ and sends to a stripper. In the stripper, the CO₂-rich amine based solution is heated to release the almost pure CO₂. Finally, the CO₂-lean amine based solution is recycled into the absorber (Howard, 1999; Howard *et al.*, 2009).

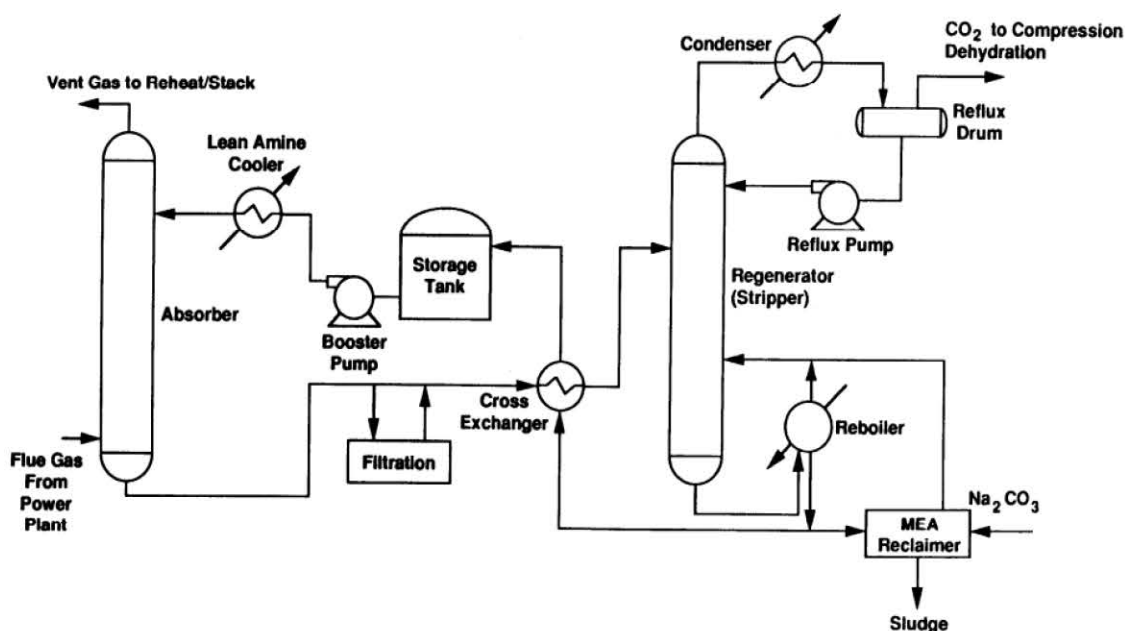


Figure 2.1: Process flow diagram of amine separation process (Howard *et al.*, 2009)

In general, the amine based solvent which was developed during the past 60 years as a nonselective solvent, is used for removing the acidic gases i.e., CO₂ and H₂S, from natural gas streams (Zhao *et al.*, 2008). However, the chemical processes associated with the degradation of the amine based solvent are still not completely understood, which leads to increases in material costs, waste disposal costs, and energy demands for the CO₂ capture process (Zhao *et al.*, 2008). In addition to the energy consumed during the absorption/desorption process, the loss of process efficiency is in the range of (11–14) % points (Göttlicher, 2006). Furthermore, the requirement of large amounts of amine based solvents in removing CO₂ molecules and the ecological aspects for the recycling of amine based solvent has yet to be fully developed (Diwekar and Shastri, 2011). Thus, another attractive alternative technique for CO₂ gas separation is the membrane technology which is introduced here (He and Hägg, 2011).

2.1.2 (b) Membrane Gas Separation

The application of the membrane technology in removing CO₂ has shown a drastic increase since their first application in 1981, especially for applications that have large flows, high CO₂ concentration, or are in remote locations (Dortmundt and Doshi, 1999). Based on Yang *et al.* (2008), the membrane gas separation is an energy saver, space efficient, and is easily scaled up. Furthermore, membrane based gas separation has the advantage of being more compact and green technology (Sanip *et al.*, 2011). Hence, the CO₂ separation using membrane technology has led to a promising future (Yang *et al.*, 2008).

There are less than 10 types of polymer materials that have been used for at least 90% of the total installed membrane-based gas separation modules, including cellulose acetate (CA), polyimide, polyaramide, polysulfone, polycarbonates, polyethersulfone, and polyphenylene oxide (Baker, 2002). Among these polymeric materials, CA membranes have been used commercially for many gas separation applications (Schell *et al.*, 1989), due to the high solubility of CO₂ and hydrogen sulfide (H₂S) within the CA-polymer matrix. However, the plasticization behavior of these membranes induces swelling, disrupts the polymer matrix, and increases the mobility of the polymer chains, thus, adversely changing the membrane characteristics required for good gas separation performance (Bernardo *et al.*, 2009).

The basic concept of the membrane separation process is demonstrated in Figure 2.2, where, the pressure or concentration gradient is frequently the driving force across the membrane-based gas separation (Ismail *et al.*, 2009). The permeation and selectivity are the most well-known basic performance

characteristics. Permeability is defined as the ability of permeants to pass through a membrane matrix. Meanwhile, selectivity is the ratio of permeability of more permeable components to that of the less permeable (Ismail *et al.*, 2009). For membrane gas separation, improving permeability and selectivity are both important targets. In addition, the membrane materials need to be thermally and chemically robust, resistant to plasticization and aging effects to ensure continual performance over a long period of time and cost effective to manufacture as standard membrane modules (Scholes *et al.*, 2008).

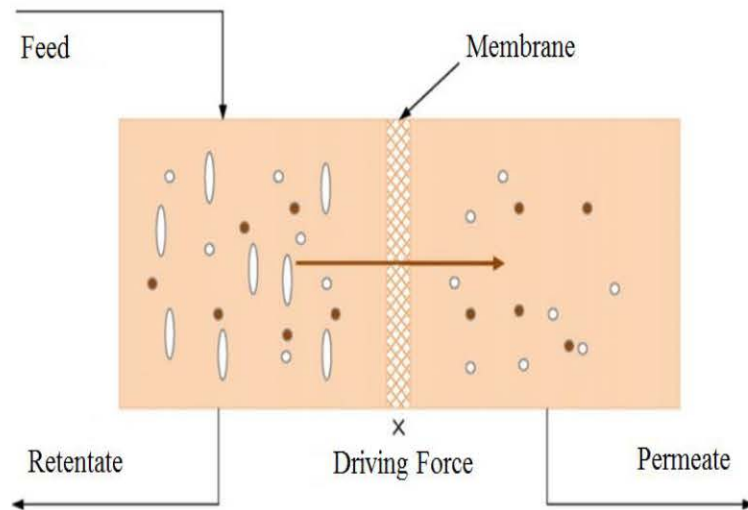


Figure 2.2: The basic concept of membrane gas separation (Ismail *et al.*, 2009)

Gas separations using polymeric membranes have achieved important commercial success in some industrial processes since the first commercial-scale membrane gas separation system was produced in the late 1970s (Wang *et al.*, 2002). Polymeric membranes were categorized based on rubbery or glassy polymers. In recent years, the glassy polymer has received a great deal of attention due to its

advantages in mechanical properties and relative economical processing capability (Ismail *et al.*, 2009).

In fact, the highly permeable membrane tends to have low selectivity, and vice versa (Scholes *et al.*, 2008). Further, the polymeric membranes suffer from thermal resistance, limited solvent and poor chemical. The occurrence of the swelling phenomena has also subsequently altered the properties of membrane separation (Goh *et al.*, 2011). Due to all these limitations, research is underway for alternative membrane material. As an alternative solution, the inorganic membrane that is synthesized from metals, ceramic or pyrolyzed carbon has attracted global interest and offers several advantages over the polymeric membrane for many gas separation processes (Goh *et al.*, 2011). However, the cost of fabrication of an inorganic membrane is high. The high investment cost can only be compensated when these kinds of inorganic membranes can achieve much higher performance relative to the polymeric membranes (Ismail *et al.*, 2009). In order to overcome the disadvantages of polymeric and inorganic membranes, a mixed matrix membrane (MMM) composed of homogenously interpenetrating polymeric and inorganic particle matrices has been introduced (Chung *et al.*, 2007).

2.2 MMM for Gas Separation

Nowadays, MMM is the new interesting approach of membrane materials for enhancing the current technology of membrane-based gas separation. Numerous worldwide academic studies have been carried out on the subject of MMM as it has shown an outstanding separation performance (Goh *et al.*, 2011).

In 1997, Zimmerman *et al.* (1997) published a pioneering literature suggesting the usage of MMM for gas separation, as the MMM provided economical and high separation performance as compared to the inorganic fillers and polymeric separation membranes (Zimmerman *et al.*, 1997). After that, several researchers have also reported the capability of MMM as an alternative approach in gas separation processes. For example, Kulprathipanja (2002) synthesized the adsorbent–polymer and polyethyleneglycol (PEG)-silicone rubber MMM. There were two types of MMMs that were synthesized. The first MMM was fabricated from silicalite-cellulose acetate (CA), NaX-CA and AgX-CA and the second MMM comprised of PEG-silicone rubber structure. In their work, the silicalite-CA MMM had demonstrated a high CO₂/H₂ selectivity of 5.15±2.2 compared to CA membrane with a selectivity of 0.77±0.06. The second MMM of PEG-silicone rubber had also proven in having a high selectivity towards the polar gases i.e., SO₂, NH₃, and H₂S (Kulprathipanja, 2002).

In recent years, Sanip and co-workers (2011) used beta-cyclodextrins (β -CD) to enhance the functionality of multi-walled CNTs (MWCNTs), which were later embedded into a polyimide membrane. The concentration effects of the functionalized MWCNTs on gas separation performances have been investigated. At 0.7 wt% loading of functionalized MWCNTs, a finger-like structure of MMM was formed and showed rapid gas diffusion within the polymer matrix. Similarly, Ismail *et al.* (2011) embedded the functionalized MWCNTs at loadings of 0.5 to 3 wt% into the polyethersulfone matrix. Their results showed that the highest gas selectivity (α) was attained from MMM with MWCNTs loading at 0.5 wt% ($\alpha_{\text{CO}_2/\text{CH}_4}$ =250.13; $\alpha_{\text{O}_2/\text{N}_2}$ = 10.65). The gas selectivity was reduced when 1 to 3 wt% of MWCNTs

loadings were used. The poorer gas separation at higher MWCNT content was probably due to the presence of interface voids within the polymer matrix. In addition, the MMMs synthesized from other inorganic fillers were summarized in Table 2.1.

Table 2.1: Summary of MMMs developed using different fillers

Reference	Polymer matrix	Filler	Type of separated gas
Li <i>et al.</i> , 2006	Polyethersulfone	Zeolite	O ₂ /N ₂
Jiang <i>et al.</i> , 2006b	Polysulfone	Zeolite	O ₂ /N ₂ & CO ₂ /CH ₄
Rafizah and Ismail, 2008	Polyethersulfone	CMS	O ₂ /N ₂
Funk and Lloyd, 2008	Poly vinyl acetate	Zeolite	O ₂ /N ₂
Gorgojo <i>et al.</i> , 2008	Polysulfone	Zeolite	H ₂ /CH ₄
Itta <i>et al.</i> , 2010	Polyetherimide	CMS	H ₂ /N ₂
Weng <i>et al.</i> , 2010	Polyphenylene oxide	CMS	H ₂ /N ₂ & H ₂ /CH ₄
Ahn <i>et al.</i> , 2011	Poly vinyl chloride	Silica	CO ₂ /N ₂ & CO ₂ /H ₂

2.2.1 Physical and Chemical Properties of MMM

In 1991, Robeson showed a plot of selectivity versus permeability, the data for many polymeric membranes, with respect to a specific gas pair, lie on or below a straight line defined as the upper bound tradeoff curve (Robeson, 1991), as shown in Figure 2.3.